Experimental study of magnetoelectric transducers for power supply of small biomedical devices

Kevin Malleron, Aurélie Gensbittel, Hakeim Talleb, Zhuoxiang Ren

EXPERIMENTAL STUDY OF MAGNETOELECTRIC TRANSDUCERS FOR POWER SUPPLY OF SMALL BIOMEDICAL DEVICES

Kevin Malleron, Aurelie Gensbittel, Hakeim Talleb and Zhuoxiang Ren

UPMC Univ. Paris 06, UR2, L2E, F-75005, Paris, France

Abstract—**This paper presents experiment results of an energy transducer based on the magnetoelectric composites. Various configurations of the layered structure composed of the Terfenol-D or/and the Metglas with the PZT-5H have been investigated. The impact of Metglas on the performance of the transducer is outlined. The high output voltage coefficient and the significant deliverable power of the combination Terfenol-D/Metglas/PZT-5H makes it as an ideal energy transducer candidate for wireless powering of embedded device in biomedical applications.**

Index Terms— **energy harvesting, magnetostrictive/piezoelectric laminate composite.**

I. INTRODUCTION

Currently, the digital "nomads" wireless technologies have attracted much attention in the international scientific community, to the point that we now speak of "Internet of Thing" (IoT). The IoT is based on the idea that identifiable objects are monitored and controlled via the Internet. To achieve this goal, it is necessary to design embedded micro-systems composed of wireless sensor nodes (WSN) while solving one of the major issues that is the excessive use of batteries in a huge number of power supplied sensors. The major concerns is that the batteries must be changed or require chargers because their limited lifetime and moreover they are made with pollutant elements which are harmful for the environment. To reduce the excessive use of pollutants while insuring the energy autonomy, the wireless sensors should be ideally supplied by energy harvesting techniques from environmental energy unpurposefully introduced or by wireless energy transmission (solution studied here) which is more appropriated when the replacement of battery is not recommended. This opens the field of self-powered or wirelessly powered low power electronic devices, which would revolutionize our society. For example, in the health domain, there is an increasing interest in developing self-powered or wirelessly powered invasive sensors to enable remote postoperative monitoring (after orthopedic or vascular surgery for instance) and to assure an instantaneous feedback on the health conditions of the patient, which is crucial for the fragile populations. In this context, a challenge to be addressed is to power wirelessly low power small biomedical devices (few 100 µW) imbedded inside a human body for a distance communication greater than 5 cm while respecting the base restrictions and the reference levels of the dosimetry standards [1].

Among the most proposed and studied solutions of the energy transmission techniques for micro-systems in biomedical domain, we find essentially transducers based on acoustic energy using piezoelectric materials or electromagnetic energy using inductive coupling between coils or RF transmission between antennas [2-3]. Use of acoustic energy is restricted by the contact between the body and the employed ultrasonic transmitter. The recoverable electromagnetic energy by inductive coupling or RF transmission for micro-systems is often low to allow a useful supply for a distance of communication greater than 5 cm. One solution to ensure an efficient wireless power transfer (at few cm of the body) would be to use a transducer device that gets simultaneously the performances of the piezoelectric material and the power transfer by the inductive coupling, such as for instance the magnetoelectric (ME) composite that combine the magnetostrictive and piezoelectric materials [4]. The composite ME materials are usually composed either of laminated bulk layers or magnetostrictive particles elements [5-6] inside a piezoelectric matrix material. The working principle of the ME transducer is as follows: under an external magnetic field composed of a harmonic magnetic field H_{ac} and a static magnetic field H_{dc}, a vibration will be excited inside the ME composite to produce a voltage between the electrodes of the piezoelectric material. In the case of laminated structures, such as the Terfenol-D/PZT/Terfernol-D for example, the ME composite exhibits a significant voltage (few volts [7][8]) under resonance condition. In this way and as shown experimentally in [9], the deliverable output power for a ME composite having dimensions 14mm (length) x 3 mm (height) x 6 mm (width) can reach few mW in matching impedance condition. Consequently, low power electronic devices can be wireless powered straightforwardly. Nevertheless, as specified the magnetostrictive layers have to be excited by an external static magnetic field H_{dc} and work around a bias point in order to maximize the ME effect. In the case of the Terfenol-D, the static magnetic bias field is relatively high (between 200Oe to 600Oe), even though in the health application, this is smaller than the authorized reference level limit of 2000Oe [1]. Moreover, as illustrated in Figure 1, for an imbedded small device, two small opposite permanent magnets may have to be envisaged to immerse a ME composite inside a uniform high static magnetic bias field.
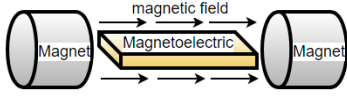
Fig. 1. Illustration of the structure using permanent magnet as static bias field.

Recent studies [10-12] propose to reduce the level of the required static magnetic bias field H_{dc} of the magnetostrictive bulk layers. It consists of adding, above or below the bulk layers, thin amorphous magnetostrictive layers having low required static magnetic bias field H_{dc} (close to 10 Oe) and high relative permeability (> 40000) such as the FeCuNbSiB or the Metglas. Those studies focus on reducing the magnetic bias by adding a thin layer at the top of their devices. In this research context, we propose to investigate experimentally the influence of the Metglas layer on ME composites Terfenol-D/PZT-5H with different configurations and compare their performances. The paper is structured as follows. The section II gives a short theoretical description of the impact of the external magnetic bias field on the mechanical stress and a simplified equivalent circuit model in linear dynamic regime. The section III introduces the studied composite ME structures and the experimental set-up. The section IV shows the measurement results in static and dynamic regimes for different ME configurations and illustrates the impact of the Metglas on the performance of the ME transducer, followed by some conclusive discussions.

II. SIMPLIFIED THEORY CONSIDERATION

Consider a bilayer composite ME shown in Figure 2 where the piezoelectric layer (P) is polarized to the transversal plan along the direction y and the magnetostrictive layer (M) is magnetized with a static magnetic bias field H_{dc} along the direction x. The relation between the stress T and the strain S inside the ME composite is given by the following constitutive law:

$$T = (c^E + c^B)S - e\,E - h(T^o, B)B \qquad (1)$$

where T^o represents a pres-stress condition (here $T^o = 0$), B is the magnetic induction, E is the electric field. e, $h(T, B)$, c^E, c^B denote respectively, the linear piezoelectric coefficient, the non-linear piezomagnetic coefficient and the stiffness tensors under constant electric field and magnetic induction, respectively.
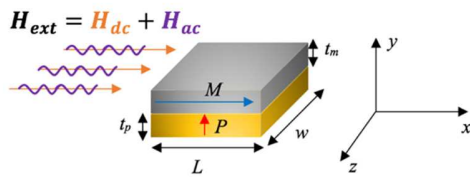

Fig. 2. Illustration of a bilayer ME composite

A. Non-linear relation between stress and magnetic induction

The term $h(T^o, B)B$ represents the induced stress T^μ due to the magnetostriction force and can be expressed as a non-linear quadratic expression of the magnetic induction B [13].

$$T^\mu \propto \lambda B^2 \qquad (2)$$

where λ represents a proportional coefficient. It is obvious that a small increase of B will lead to a large increase of the stress T^μ.

Consider now, the case illustrated in Figure 3 namely a magnetostrictive thin layer of high permeability (Metglas for example) placed above a magnetostrictive bulk layer of lower permeability (Terfenold-D for example). The induced effective stress inside the global volume depends on when the optimal static magnetic bias fields H_{dc} of the magnetostrictive thin layer and bulk layer are reached. Because of the high permeability of the thin Metglas layer, the magnetic induction in the thin layer will be much more important than in the bulk layer. This will increase significantly the mechanical stress of the thin layer according to the relation (2) as illustrated in Figure 3, and consequently improve the magnetoelectric coefficient of the transducer.

Further, if the Metglas is placed between the bulk Terfenold-D layer and the piezoelectric layer, it will concentrate the stress near the piezoelectric layer and improve the mechanical energy transfer. In other word, the Metglas concentrates the induction magnetic flux and the mechanical stress to create a more important volume stress on the PZT-5H.
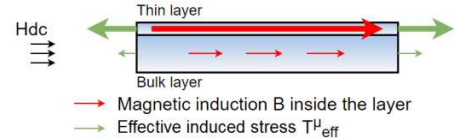

Fig. 3. Illustration of the magnetostrictive thin layer effect on a magnetostrictive bulk layer

B. Linear consideration in dynamic regime

Under the assumption of small signal dynamic field H_{ac} around the selected static magnetic bias field H_{dc}, the term $h(T^o, B)B$ can be linearized as a simple coefficient h. The equivalent circuit model of the ME composite in Figure 2 in resonance regime can be represented by the well-known Mason model as shown in Figure 4 [14].
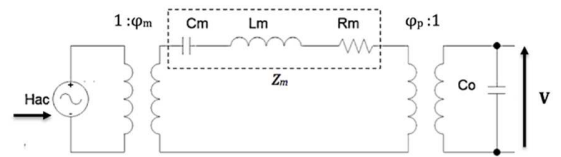

Fig. 4. Mason model of the ME composite under resonance

The impedance Z_m represents the mechanical part in which C_m, L_m and R_m are respectively the mechanical stiffness, the mass and the mechanical damping. The electrical part is represented by the clamped capacitor C_o of the piezoelectric element. The coefficients φ_m and φ_p are transformer ratios symbolizing the magnetomechanical and electromechanical coupling coefficients [15]. The parameter to predict the performance of ME composites is given by the ME voltage coefficient α_V i.e. the transfer function [14]. When a impedance electrical load Z_{load} is connected between the electrodes of the piezoelectric, α_V is given by:

$$\alpha_V = \left| \frac{V_{pp}}{H_{ac}} \right| = \left| \frac{\frac{\varphi_p{}^2}{jC_o\omega}}{\frac{\varphi_p{}^2}{jC_o\omega} + Z_{load}} \right| = \left| \frac{\varphi_p{}^2}{\varphi_p{}^2 + jZ_{load}C_o\omega} \right| \qquad (3)$$

where V_{pp} is the peak-to-peak output voltage and ω is the pulsation of the dynamic signal H_{ac}.

The resonance frequency of the composite ME corresponds to the mechanical resonance frequency defined by the following relation [4]-[12]:

$$f_r = \frac{1}{2L} \sqrt{\frac{\overline{Y}}{\overline{\rho_v}}} \qquad (4)$$

where L, $\overline{Y}$ and $\overline{\rho_v}$ are, respectively, the equivalent length, the averages of the Young modulus and the mass density of the layered transducer, which can be analytically determined.

III. ME SAMPLES AND EXPERIMENTAL SET-UP

The measurements were carried out, respectively, on both the bilayer and trilayer structures with four different combinations: two combinations for the bilayer structure, PZT-5H/Metglas and PZT-5H/Terfernol-D; and two combinations for the trilayer structure, PZT-5H/Metglas/Terfernol-D, PZT-5H/Terfernol-D/Metglas as represented in Figures 5(a) and 5(b), respectively. The dimensions of magnetostrictive layers are $t_{m1} = 1\ mm$, $L_m = 14\ mm$, $w = 10\ mm$ for Terfenol-D and $t_{m2} = 35\ \mu m$, $L_m = 14\ mm$, $w = 10\ mm$ for Metglas. Both layers are poled along the longitudinal direction. For the PZT-5H, the dimensions are $t_p = 1\ mm$, $L_p = 20\ mm$ and $w = 10\ mm$ for all configurations. Its surfaces are covered with 3μm thick Au electrodes and it was poled along the transversal direction. The mechanical-electric-magnetic properties and parameters of the different materials are given in the Appendix.

The length of the PZT-5H is chosen longer than the magnetostrictive layers in order to connect conveniently the electrical impedance load Z_{load} that represents symbolically the input impedance of an electronic device it supplies. Otherwise, this emplacement could be used to put the electronic device. To guarantee the continuity of the mechanical coupling between each material interface contact, the adjacent layers have been bonded conjointly with an epoxy resin (SADER epoxy progressive) under a pre-stress during 24 hours.
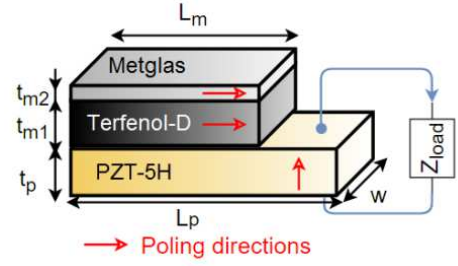
(a) Samples PZT/Terf (without the top Metglas) and PZT/Terf/Met.
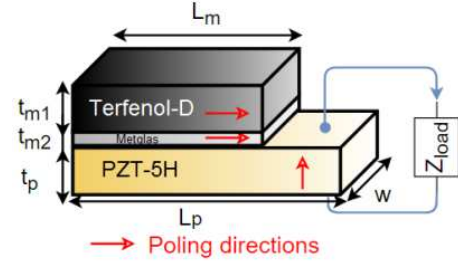
(b) Samples PZT/Met (without the top Terfenold-D) and PZT/Met/Terf

Fig. 5. The studied trilayer ME composites

The electrical model of the ME composite in Figure 4 can be simplified by the equivalent Thevevin circuit represented in Figure 6 [16]. The external equivalent generator, namely V_{in} is equals to the output voltage in open circuit condition ($Z \rightarrow \infty$) and the impedance Z_i represents the internal impedance of the ME layers.
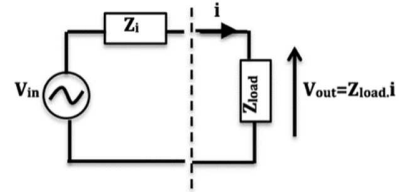

Fig. 6. The simplified equivalent circuit of a ME composite

The deliverable output power is maximal under matching condition, i.e. when the external electrical load Z_{load} is equals to the real part of internal impedance $R_i = \mathrm{re}(Z_i)$. In this case, the output voltage V is equals to $V_{in}/2$. Thus, the deliverable output power P_{rms} is extracted as:

$$P_{rms} = \frac{\left(\frac{V_{in}}{2}\right)^2}{R_i} \qquad (5)$$

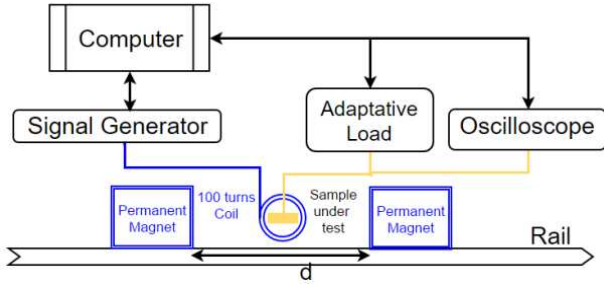The schematic of the experimental set-up is presented in Figure 7.

Fig. 7 Experimental Set-up.

During the measurements, the ME transducer was placed inside a cylinder region of 10 mm diameter and 20 mm long. To acquire the small harmonic magnetic field H_{ac} a coil with 100-turn of Cu wire (0.2 mm diameter) was wrapped around the ME composite and the driving field H_{ac} has been created by a harmonic ac current generated with an arbitrary waveform generator (Rohde & Schwarz HM8150). A control loop ensures the ac current inside the coil to generate the desired rms of the ac magnetic field at each frequency step. The uniform static magnetic field 30-1600 Oe was obtained by adjusting the distance d between the permanent magnets along a moving rail. The calibration between the distance d and the magnitude of the static magnetic field has been controlled by a Gaussmeter in the middle of the cylinder region. The peak-peak output voltage has been measured with a digital oscilloscope (Keysight MSO7054A) with the input impedance 1 MΩ. A photoresistor controlled by LED has been used as a pure resistive adaptive load Z_{load} to extract the internal impedance of the composite ME at each frequency step. Each adjustment and data acquisition had been achieved automatically under a computer driven with a Matlab® program.

IV. MEASUREMENTS AND DISCUSSIONS

### A. Measurement of optimal static magnetic bias field

In order to obtain the optimal static magnetic bias field H_{dc}, the ME coefficient α_E has been measured in low frequency (at 1 kHz) while imposing the harmonic magnetic field H_{ac} at 6 Oe. Figure 8(a) and 8(b) present the measurement results of all four configurations for the normalized ME coefficient $\alpha_E = \alpha_V/t_p$ in function of the static magnetic bias field. Comparison of measurements between the bilayer and the trilayer structures shows the influence of the thin Metglas layer. As expected, the PZT/Metglas sample presents a high magnetoelectric static coefficient in low field, while the PZT/Terfenol-D sample present it in a higher static field (results summarized in table 1). In the low field, we can see the influence of the Metglas leading to a local maximum for the PZT/Terf/Met and PZT/Met/Terf samples.

As for the trilayer structures, we see that the PZT/Terf/Met sample is slightly better that the PZT/Terf sample. This shows that the Metglas layer improves slightly the mechanical transfer. But the optimal static bias field remains the same with or without Metglas. On the contrary, the PZT/Met/Terf

sample presents a lower static α_E at the frequency 1kHz and the optimal bias field is a little bit higher. It can be noticed that this study allows determining where the optimal static magnetic bias field occurs and the ME coefficients do not have much sense because the transducer is not under the resonance.
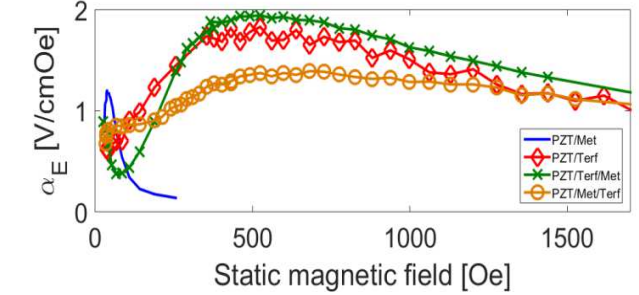
(a) Static magnetoelectric coefficients for a high static magnetic field.
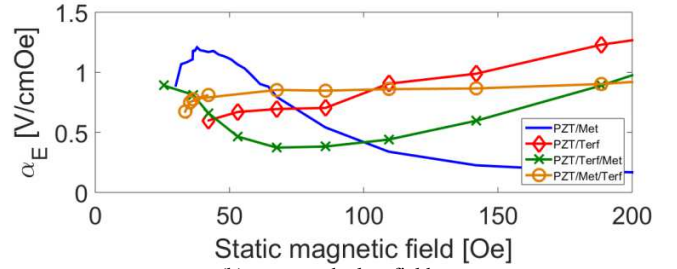
(b) zoom on the low fields.

Fig. 8. Static magnetoelectric coefficients

Sample	Optimal static field [Oe]	α_E [V/cmOe]
PZT/Metglas	38	1.2
PZT/Metglas/ Terfenol-D	682	1.4
PZT/ Terfenol-D	525	1.8
PZT/ Terfenol-D /Metglas	525	2

Table 1. Optimal static bias field (ref. Fig. 8) at 1 kHz.

B. Dynamic measurements

Figure 9(a) and 9(b) show dynamic responses of the ME coefficient α_E for all cases for a dynamic field H_{ac} at 1 Oe under the optimal static field shown in Table 1. The resonances frequencies as well as the pick value of α_E are indicated in Table 2. The resonance frequency is chosen as the frequency which exhibits the highest ME coefficient. In figure 9(a), we assume that the second peak corresponds to another mode of the material created by the difference of length between the piezoelectric and the magnetoelectric phases. In figure 9(b), this second peak is hidden by the quality factor.

This measurement confirms that the bilayer PZT/Metglas present the lowest magnetoelectric coefficient while the PZT/Terf is much higher.

The sample PZT/Met/Terf has lower ME coefficient α_E and higher bias field in the previous low frequency measurement. However, it presents the highest α_E in dynamic under the resonance. This confirms that the Metglas layers concentrate

the stress around the piezoelectric layers.

On the other hand, the trilayer PZT/Terf/Met is better than the bilayer PZT/Terf in low frequency measurement. In dynamic regime, those two samples seem equivalent which shows that the effect of the Metglas layers added on the top of a sample does not improve the ME coefficient.
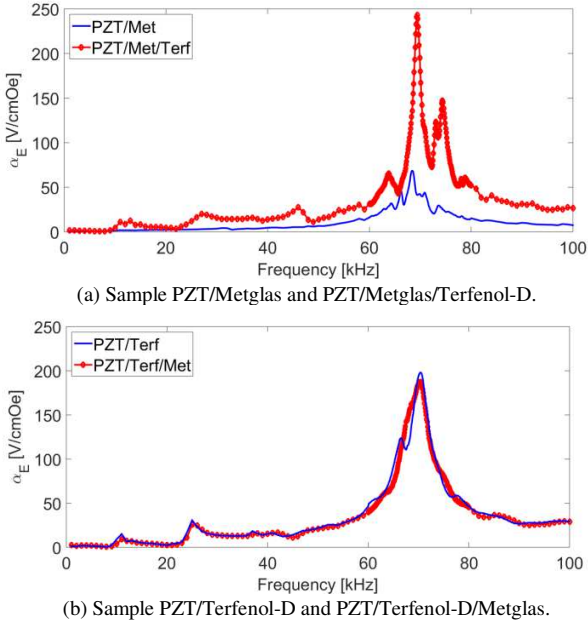

(a) Sample PZT/Metglas and PZT/Metglas/Terfenol-D.

(b) Sample PZT/Terfenol-D and PZT/Terfenol-D/Metglas.

Fig. 9. Frequency dependence of the normalized ME coefficient α_E

Sample	Resonance Frequency [kHz]	α_E [V/cmOe]
PZT/Metglas	68.4	68.6
PZT/Metglas/Terfenol-D	69.4	243
PZT/ Terfenol-D	70.4	198
PZT/ Terfenol-D /Metglas	70.4	187

Tab.2. Summary of dynamic magnetoelectric coefficient for each sample.

C. Discussions

The resonance frequency of the transducer calculated by (4) is 70 kHz. Compare with the measured resonance frequencies shown in Table 2, slight shifts are observed. Those shifts are due to the influence of the resin epoxy in the global Young's modulus [4]-[12] as well as the variances between the real material properties and those considered in the modeling.

Table 3 shows the measurement results of the internal impedance performed in according to the procedure mentioned in section III. The internal impedance of each ME composite sample is smaller than which of the PZT layer. This result is due to the mechanical damping from the magnetostrictive layers [18]. Figure 10 presents the frequency dependence of the deliverable output power. We can notice that the Metglas improves significantly the deliverable output power of the sample PZT/Met/Terf in exhibiting a high power close to 600µW.

Sample	Resonant Frequency [kHz]	$R_i[\Omega]$
PZT only	67.5	1272
PZT/Met	68.4	353
PZT/Met/Terf	69.4	342
PZT/Terf	70.4	361
PZT/Terf/Met	70.4	339

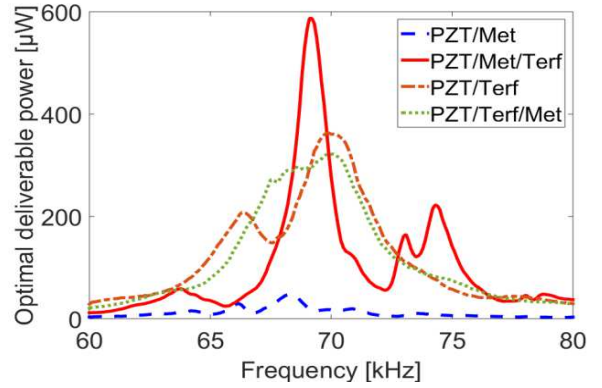Tab.3. Internal impedance for each sample under resonance

Fig.10. Frequency dependence of the P_{rms}.

D. Potential application in biomedical domain

Consider a biomedical sensor chip that works with a power requirement of 0.6 mW, in this case the main advantages (illustrated in Figures 11 and 12) to use the proposed composite ME PZT/Metglas/Terfenol-D are:

- Possible incorporation with a minimally invasive (a medical catheter for instance).

- Low specific absorption by the human body for frequencies lower than 100 kHz delivered by a distant external source.
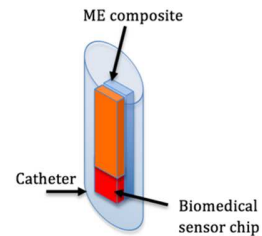

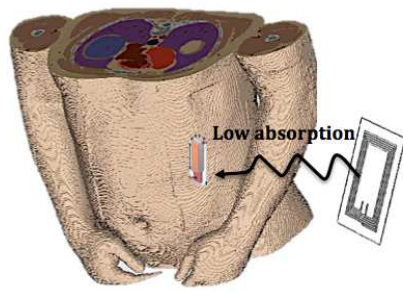Fig.11. Illustration of the ME composite into a catheter

Fig.12. Wireless powering illustration of the ME composite inside a body

V. CONCLUSION

In this experimental study it is shown that adding a Metglas layer between the PZT-5H and the Terfenol-D improves significantly the output voltage as well as the deliverable output power in resonance regime. The low working frequency and the low magnetic field magnitude respecting the reference level of the dosimetry standards [1] as well as the small dimensions of the ME composite are propitious to design ME energy transducer for wireless powering of embedded electronic devices in biomedical domain. The experiment results presented in this paper will be explored in the future work to establish appropriate models that can be integrated in circuit simulators (VHDL-AMS, VerilogA, Spice) for the design and optimization of ME based energy transducers.

VI. APPENDIX

Properties materials:
PZT-5H :
Young's module (E)= 6.09×10^{10} N.m^{-2}
Density (ρ) = 7750 kg.m^{-3}
Terfenol-D:
Young's module (E)= 2.27×10^{10} N.m^{-2}
Density (ρ) = 9250 kg.m^{-3}
Relative permeability: $\mu_{31} = \mu_{33} = 9.3$
Metglas:
Young's module (E)= 10×10^{10} N.m^{-2}
Density (ρ) = 7180 kg.m^{-3}
Relative permeability: $\mu_{31} = \mu_{33} = 15000$

REFERENCES

[1] International Commission on Non-Ionizing Radiation Protection (ICNIRP), http://www.icnirp.org

[2] S. H. Song, A. Kim and B. Ziaie, "Omnidirectional Ultrasonic Powering for Millimeter-Scale Implantable Devices," in *IEEE Transactions on Biomedical Engineering*, vol. 62, no. 11, pp. 2717-2723, Nov. 2015.

[3] Basaeri, H., Christensen, D., Roundy, S., 2016. "A Review of Acoustic Power Transfer for Bio-Medical Implants", Smart Materials and Structures. 25.12 (2016): 123001

[4] H. Talleb and Z. Ren, "Finite element modeling of a magnetoelectric energy transducer including the load effect", *IEEE Trans. on Magn*, vol. 51, issue 3,2015

[5] R. Corcolle, L. Daniel and F. Bouillault, "Generic formalism for homogenization of coupled behavior: Application to magnetoelectroelastic behavior", *Physical Review B*, 78, 214110 (2008).

[6] H. Talleb, A. Gensbittel, Z. Ren, "Multiphysic modeling of multiferroic artificial materials by the finite element method", European Physical Journal Applied Physic.

[7] P. Record, C. Popov, J. Fletcher, E. Abraham, Z. Huang, H. Chang, R.W. Whatmore, Direct and converse magnetoelectic effect in laminate bonded Terfenol-D–PZT composites, In Sensors and Actuators B: Chemical, Volume 126, Issue 1, 2007, Pages 344-349, ISSN 0925-4005.

[8] Shuxiang Dong, Jinrong Cheng, J. F. Li, and D. Viehland, "Enhanced magnetoelectric effects in laminate composites of Terfenol-D/Pb(Zr,Ti)O3 under resonant drive", Applied Physics Letters 2003 83:23, 4812-4814.

[9] Y. Wang, X. Zhao, J. Jiao, L. Liu, W. Di, H. Luo, S. Wing, "Electrical resistance load effect on magnetoelectric coupling of magnetostrivtive/piezoelectric laminated composite", Journal of Alloys and Compounds , 500, 2010, pp. 224-226.

[10] L. Chen, P. Li, Y. Wen, Y. Zhu, "Large self-biased effect and dual-peak magnetoelectric effect in different three-phase magnetostrictive/piezoelectric composites", Journal of Alloys and Compounds, Volume 606, 2014, Pages 15-20, ISSN 0925-8388.

[11] Chen, P. Li, Y. Wen and Y. Zhu, "Near-Flat Self-Biased Magnetoelectric Response in Three-Phase Metglas/Terfenol-D/PZT-Laminated Composites," in IEEE Transactions on Magnetics, vol. 51, no. 11, pp. 1-4, Nov. 2015.

[12] X. Xu, J. Qiu, Y. Wen, P. Li, H. Chen and X. Liu, "Zero-Biased Magnetoelectric Effects in Five-Phase Laminate Composites With FeCoV Soft Magnetic Alloy," in IEEE Transactions on Magnetics, vol. 51, no. 11, pp. 1-4, Nov. 2015.

[13] Thu Trang Nguyen, Frederic Bouillault, Laurent Daniel and Xavier Mininger, "Finite element modeling of magnetic field sensors based on nonlinear magnetoelectric effect", Journal of Applied Physics,109, 084904 , 2011

[14] S. Dong, J-F. Li and D. Viehland, "Longitudinal and transverse magnetoelectric voltage coefficients of magnetostrictive/ piezoelectric laminate composite: experiments," in IEEE Transactions on Ultrasonics, Ferroelectrics, and Frequency Control, vol. 51, no. 7, pp. 794-799, July 2004.

[15] Hao-Miao Zhou et al 2013 Smart Mater. Struct. 22 035018

[16] K. Malleron, H. Talleb, A. Gensbittel and Z. Ren, "Finite-Element Modeling of Magnetoelectric Energy Transducers With Interdigitated Electrodes," in IEEE Transactions on Magnetics, vol. 53, no. 6, pp. 1-4, June 2017.

[17] Smith, A., Wilkinson, S. J., & Reynolds, W. N. (1974). The elastic constants of some epoxy resins. Journal of Materials Science, 9(4), 547-550.

[18] M. Brissaud, "Matériaux piézoélectriques: caractérisation, modélisation et vibration", PPUR presses polytechniques, 2007.